Steady-state pressure drop and heat transfer in He II forced flow at high Reynolds number

S. Fuzier[1,2], B. Baudouy[3] and S. W. Van Sciver[1,2]

[1]National High Magnetic Field Laboratory
1800 E. Paul Dirac Drive, Tallahassee FL 32310, USA
[2]Mechanical Engineering Department
FAMU-FSU College of Engineering
[3]CEA/Saclay, DSM/DAPNIA/STCM
91191 Gif-sur-Yvette Cedex, France

Abstract

An experiment to study forced flow superfluid helium (He II) at high Reynolds number has been recently developed at the NHMFL. The liquid is pushed from a bellows pump through a 1m long, 9.8 mm inside diameter smooth tube test section to attain a maximum velocity of 18 m/s and a Reynolds number up to 2×10^7. The test section is instrumented with eight bare chip thermometers, a heater and a differential pressure transducer. Measurements of pressure drop have been performed to determine the friction factor for Reynolds number exceeding 10^7. These are compared to results from previous forced flow experiments at lower velocities and to some existing correlations. The temperature rise in He II forced flow, due to the isenthalpic expansion in the test section, has also been measured for velocities between 0.5 m/s and 16 m/s. These temperature profiles are related to the Joule-Thomson coefficient. The heater, positioned in the middle of the test section, allows heat transfer measurements and can be used as a thermal flow meter.

Keywords: superfluid helium, forced flow, heat transfer

Nomenclature

C_p	Specific heat at constant pressure (J/kg.K)
D	Diameter (m)
f	Fanning friction factor

$f^{-1}(T)$ Turbulent He II heat conductivity function ($W^3/m^5.K$)

H Enthalpy (J/kg)

$\dot{m}$ Mass flow rate (kg/s)

L Length (m)

P Pressure (Pa)

q Heat flux per cross section area (W/m^2)

q_l Heat flux per unit volume (W/m^3)

Re Reynolds number

T Temperature (K)

v Velocity (m/s)

α Thermal expansion coefficient (K^{-1})

η_n Viscosity of the normal fluid ($N.s/m^2$)

μ_j Joule-Thomson coefficient (K/Pa)

ρ Density (kg/m^3)

ε Roughness (m)

Introduction

Superfluid helium is often selected as a coolant for superconducting magnets because of its exceptional thermal properties and low operating temperature enhancing the performance of the superconductors. Many magnets are cooled in a static bath of He II, either saturated or pressurized. Forced flow superfluid helium, already used to cool fusion magnets[1] and spaced based magnets[2] is worth considering in the design of general superconducting magnets[3]. This method indeed enhances the cooling abilities of the fluid, but the pressure drop in the flow lines induces a temperature increase of the helium due to Joule-Thomson effect. The design of these systems, with high Reynolds number or long circulation paths, requires the consideration of forced flow He II fluid dynamics, heat transfer and the Joule-Thomson effect. Several forced flow experiments[4,5,6] have been built to investigate mainly these two first aspects for flow velocities up to 5.4 m/s. The

present experiment can produce forced flow up to 18 m/s, giving access to Reynolds number in the 10^7 range. This paper presents the experiment and steady-state results of pressure drop, Joule-Thomson effect and heat transfer in this high Reynolds number regime.

Experiment

The present experiment is composed of a can/bellows pump assembly which generates the motion of He II through the instrumented experimental loop (Fig 1). The can/bellows pump assembly contains a 0.28 m diameter bellows with a 0.3 m stroke actuated by a stepper motor (model ETS80-B04LA41-GF343-A manufactured by Parker Motion and Control) capable of creating a maximum mass flow rate of 0.21 kg/s for a duration of 11 s. The bellows is located in a 80 liter can containing a buffer volume of saturated He II for receiving the return flow and refilling the bellows. This assembly is suspended in the vertical part of the Cryogenic Helium Experimental Facility (CHEF), which consists mainly of a 0.6 m ID, 3.65 m long horizontal clear bore. It is equipped with large hinged cover for work access inside the cryostat and a vertical stack presently containing the can/bellows pump. The isothermal radiation shields are cooled by natural convection loops at 4.2 and 77 K from reservoirs of cryogens residing in the vertical section. The experimental flow loop is supported on a rail system along the top of the inner most shield located in the horizontal part of the cryostat.

The main part of this experimental loop (Fig. 2) is a 1.23 m long, 9.8 mm inside diameter straight stainless steel tube mounted with instrumentation modules, which can be used to insert thermometers or heaters. Before the first module, a 0.2 m entry length allows the stabilization of the flow. The return line is made of 76 mm inside diameter pipe to minimize the pressure drop in the experiment.

The test section contains eight bare chip Cernox thermometers and one ceramic packaged. The packaged sensor is used for reference for *in situ* calibration. The sensors are mounted on delrin supports inserted in the instrumentation modules. The chips are positioned on the tip of these supports, which are in direct contact with the flow and have

been machined to match the shape of the pipe to minimize flow disturbance. With these thermometers, the absolute temperature can be measured with a precision of $\pm$ 5 mK

The pressure drop is measured across a 1 m length part of the test section starting after the 20 cm entrance flow stabilization length. A cold differential pressure transducer (model DP 10, Validyne Engineering Corporation) is used with its signal conditioning electronic package. The proximity of the transducer wires with other signals cables affects its output, so these paired wires have been independently shielded and separated from the other cables. The transducer has been calibrated outside the experiment for temperatures of 1.7, 1.85 and 2 K and the output value corresponding to no pressure difference has been subtracted to compensate for zero shifts.

A heater is located in the middle of the test section. It is made of 1.82 m of 54.9 Ω/m Nichrome wire coiled and positioned laterally in contact with the He II.

Experimental data were recorded digitally for a duration including the stroke and a few seconds preceding and following it. The measurements before the stroke are used for reference of bath temperature and pressure drop. Stroke durations were between 11 s for the highest speed and 360 s for the lowest. For the heat transfer measurements, the heater was powered in the middle of the stroke to let the flow stabilize before and have a reference with no heat applied. The data presented correspond to the average of the sensors output for a few seconds.

Results

In the present set of experiments, the pressure drop was recorded in the test section between the location of the first and the last thermometers, which are 1 m apart after the 0.2 m stabilization length. These results, corresponding of flow velocities between 6 and 14 m/s and a bath temperature of 1.7 K, are use to determine the Fanning friction factor $f = \frac{\pi^2 D^5 \rho \Delta P}{32 \dot{m}^2 L}$ and plotted versus the Reynolds number $\mathrm{Re} = \frac{\rho v D}{\eta_n}$ in Fig. 3. This graph shows also results from some previous experiments of forced flow in pipes of various dimensions. Kashani[4] measured pressure drop on a 2 m copper loop of 3 mm inside diameter for velocities between 0.4 and 0.9 m/s. Walstrom[7] et al carried

measurements in a copper loop of 4.6 m for velocities between 2 and 5.4 m/s and in a 4.1 m straight tube. All these data were taken at 1.8 K. These results are compared with two correlations for classical fluid turbulent flow. The Von Karman-Nikuradse smooth tube correlation[7]

$$\frac{1}{\sqrt{f}} = 1.737 \ln\left(\mathrm{Re}\sqrt{f}\right) - 0.396 \qquad (1)$$

is typically used for Reynolds number between 4000 and 3×10^6. A correlation from Colebrook[8]

$$\frac{1}{\sqrt{f}} = -4\log\left(\frac{\varepsilon}{3.7D} + \frac{1.25}{\mathrm{Re}\sqrt{f}}\right) \qquad (2)$$

is used for flow of Reynolds number between 4×10^3 and 10^8 and includes the relative surface roughness $\frac{\varepsilon}{D}$. We selected $\frac{\varepsilon}{D} = 1.4\times10^{-4}$, which is a published value for drawn tubing corresponding to the dimensions of the test section[8]. Our data are of the same order of magnitude but higher than this correlation. This difference is probably due at least in part to the presence of the thermometers positioned on the side of the test section in contact with the flow. Even with the delrin supports machined to match the shape of the pipe, the penetration still represents some deviation from a completely smooth tube. These additional pressures losses are included in our calculations of the Fanning friction factor, which corresponds normally to uniform pipes.

The warming of the superfluid helium due to the pressure drop in the test section during the forced flow has been measured in eight locations for velocities between 0.52 and 16.6 m/s. The resultant temperature profiles are shown on Figure 4. On this graph, the zero on the x-axis corresponds to the end of a flow divergence, and the beginning of the 9.8 mm ID test section. Similarly the end of this axis corresponds to the end of the test section and the beginning of a divergence to the large diameter return pipe. By construction, the temperature in these two extremities should be close to the bath temperature.

The temperature increases along the pipe and with increasing flow velocity. This result can be related to the Joule-Thomson coefficient, $\mu_j = \left(\frac{\partial T}{\partial P}\right)_h = \frac{\alpha T - 1}{\rho C_P}$. The term $\frac{\alpha T}{\rho C_p}$ corresponds to the reversible or isentropic part of the temperature change associated with an expansion but is negligible for He II compared to its irreversible counterpart $\frac{-1}{\rho C_p}$ except near T_λ [9]. Thus, since ρ ~ constant and $C_p \sim T^{5.6}$ for He II in this temperature regime, then $\mu_j \sim T^{-5.6}$. Using the pressure drop data and assuming the local pressure gradient equals the average pressure gradient, i. e. dp/dx = Δp/Δx, then the temperature profile in Fig. 4 should display a gradually decreasing slope along the channel. For example, the slope at 1.85 K should about 62% of the value at 1.7 K. The experimental results display a decreasing slope, but the magnitude of the effect is larger than can be explained by variations in μ_j. Further, the slope decrease does not appear to be monotonic suggesting the possibility of non-constant pressure gradient. This effect may be related to the variations in the pressure gradient measured in the experiment (and discussed below). Figure 5 shows the difference of temperature measured between the last and the first thermometer versus the pressure drop measured between the two same locations for flow velocities between 6.22 m/s and 14.50 m/s. These temperature differences are compared to $\mu_j \Delta P$, the line in Fig. 5 which are the temperature differences associated with the Joule-Thomson coefficient.

Figure 6 shows typical heat transfer measurements for a flow velocity of 0.52 m/s and different heater powers. On this graph, the heater is located at x = 0.684 m. Most of the heat is carried downstream of the heater by ordinary convection which explains the overall higher temperature for x > 0.684 m. However in He II, some heat is also carried upstream by internal convection resulting in the concave shape before the heater. The lines correspond to a numerical solution to the steady state He II forced flow heat transfer equation[4]:

$$\rho v C_P \frac{dT}{dx} - \frac{d}{dx}\left[f^{-1}(T) \frac{dT}{dx} \right]^{\frac{1}{3}} = q_l(x) \qquad (3)$$

where v is the velocity of the flow, q_l the heater power locally injected by unit volume of liquid. It should be noted that this model does not include effects due to pressure variations. For the temperature dependence of the physical properties, a polynomial expression is used for the heat conductivity[10] and a polynomial fit of the values of the software HEPAK® are used for the heat capacity. The equation is integrated once analytically and solved with a Runge-Kutta 4 method using the values of the first and the last thermometer as boundary conditions. The two extremities of the test section could have been used instead, but even if by experimental construction their temperatures should be close to the bath temperature, they are not known precisely, as no thermometers are located there. The model is in good agreement with the experimental results.

Similar results are shown in Fig. 7 for a flow velocity of 4.14 m/s. The computed temperature profile solution of Eq. 3 is systematically below the experimental results. One possible cause for this result is that the model does not include pressure driven isenthalpic expansion (Joule-Thomson effect). It should be mentioned that for this graph, the boundary conditions used are a fixed temperature boundary at the first thermometer and a zero temperature gradient at the last thermometer ($dT/dx = 0$ at $x = 1.184$ m). Indeed, the temperature profile down stream of the heater is nearly flat due to the dominance of ordinary forced convection over internal convection at this high velocity as can be see in the data. It can also be seen that the internal convection acts in a small distance upstream the heater and from the experimental points downstream the heater and the geometry of the experiment, we expect that the internal convection downstream the heater acts principally after the last thermometer. Due to the dominance of the ordinary forced convection term in Eq. 3 at this high velocity, a reasonable change in this last boundary condition only affects the computed temperature solution locally near this last point but not the overall profile. As the computed profile downstream the heater is bellow the experimental data, the gradient boundary condition at the last thermometer is preferred to the fixed point boundary condition as the latter produces a rising temperature profile near this last point to meet its value, which has no physical meaning. The fact that the profile is lower than the experimental data may be an illustration of the limitations of our model for flow velocities where the Joule-Thomson effect is significant.

The heater can also, to a certain extent, be used as a thermal flow meter[6] (Figure 8) using the approximate formula $v \approx \frac{q}{\rho \times \Delta H}$ where q is the heat generated at the heater per cross sectional area and ΔH the difference of enthalpy of the helium just downstream the heater location before and after the heat power is turn on. Figure 8 shows the ratio between the velocity given by the displacement of the bellows and the velocity computed by this method for different heat powers. The measurement on the thermometer just following the heater and positioned in x = 0.735 m is used for the determination of the enthalpy. This method is more appropriate for high velocities when the heat carried by internal convection is negligible over the heat carried by ordinary convection. The accuracy is poor for v = 0.52 m/s and within 20 % for v = 4.14 m/s. It should improve again for higher velocities but unfortunately, we could not study these regimes because of limitations to the total heat applied.

Figure 9 shows the time-dependent evolution of the pressure drop in the test section. For the three cases illustrated, the compression of the bellows starts at t = 5 s and occurs at constant rate. For v = 6.22 m/s, a constant pressure drop is observed for the entire cycle. But for velocities starting around 10 m/s and above, we observe some instabilities which are very repeatable for different runs. In Fig. 9, these instabilities are most pronounced for v = 12.44 m/s where a clear transition to a higher pressure drop occurs after 8 s. For higher velocities the profiles transition earlier to a quasi-constant value. The reason for these instabilities is still unresolved at this point and we plan to do some absolute pressure measurements in the test section to help clarify this issue. The eventual relationship between these time-dependent instabilities and possible non-uniformities in the pressure gradient will also be studied.

Conclusion

A forced flow He II experiment has been built to investigate fluid mechanics and heat transfer for Reynolds number up to the 10^7 range. The pressure drop appears to follow classical correlations. The warming of He II due to an isenthalpic expansion

(Joule-Thomson effect) has been observed for various velocities. Heat transfer measurements have been made and compared with a classical He II model, which does not take into account pressure effects. The model corresponds well to the experimental data for v = 0.52 m/s. For v = 4.14 m/s, the models does not match as well which seems to confirm that pressure effects becomes significant in the heat transfer process for higher velocities. The instabilities of the pressure drop signal are under further study.

Acknowledgements

The authors are grateful to Scott Maier for his help during the assembly of the experiment and Dr. Mike Smith for his significant contribution in the design process and the programming of the experimental Labview® interface. This work is supported by the Departement of Energy – Division of High Energy Physics under grant FG02-96ER-40952.

References

1. Hofmann, A. in *Proceedings of the 11th International Cryogenics Engineering Conference*, Butterworths, London, 1986, 306
2. Green M.A. Cryogenics: its influence on the selection of the ASTROMAG superconducting magnet coils. *Cryogenics*, 1990, **30**, 178.
3. Van Sciver S.W. Forced flow HeII cooling for superconducting magnets-design considerations. *Cryogenics*, 1998, **38**, 503.
4. Kashani A. Ph.D. Thesis, University of Wisconsin-Madison 1986
5. Walstrom P.L. Heat transfer by internal convection in turbulent HeII forced flow. *J. Low Temp. Phys.*,1988, **73**, 391.
6. Rousset B., Claudet G., Gauthier A., Seyfert P., Martinez A., Lebrun P., Marquet M., Vanweelderen R. Pressure drop and transient heat transport in forced flow single phase helium II at high Reynolds number. *Cryogenics*, 1994, **34** Suppl. ICEC, 317.
7. Walstrom P.L., Weisend II J.G., Maddocks J.R. and Van Sciver S.W. Turbulent flow pressure drop in various He II transfer system components. *Cryogenics*, 1988, **28**,101.
8. Munson B.R., Young D.F., Okiishi T. H. *Fundamentals of fluid mechanics*, second edition, John Wiley&Sons, 1994, 488
9. Huang B.J., Joule-Thomson effect in liquid He II. *Cryogenics*, 1986, **26**, 475.
10. Van Sciver S.W. *Helium Cryogenics*, Plenium Press, New York, 1986, 144.

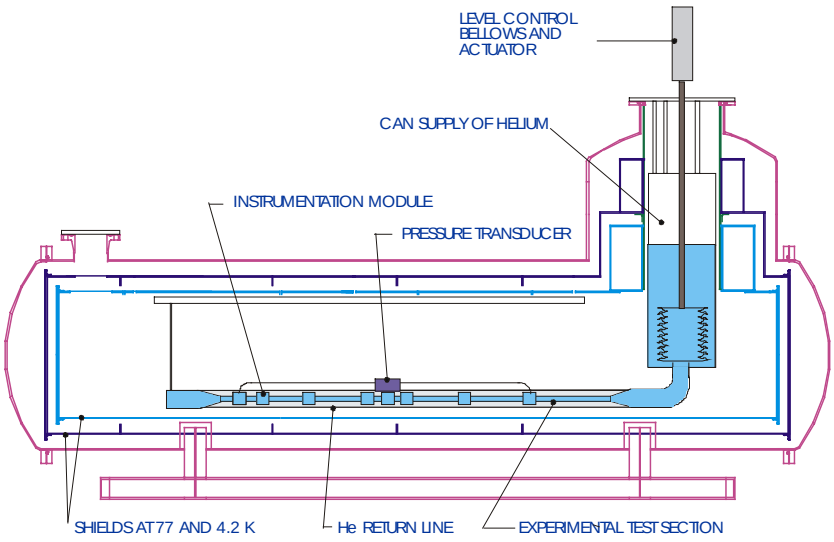

Fig.1: Schematic of the experiment

Fig.2: Experimental loop for He II forced flow

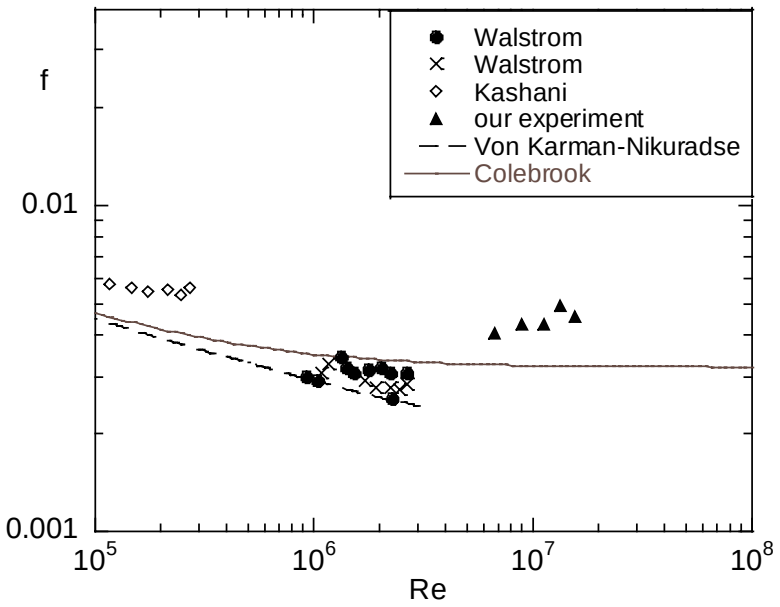

Fig.3: Friction factor data for turbulent flow of He II for this and previous experiments.

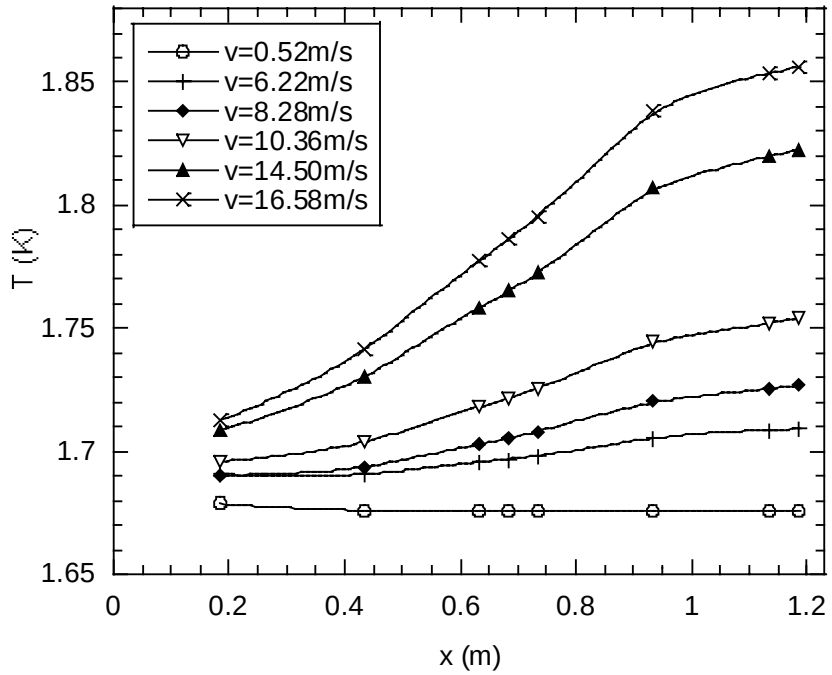

Fig.4: Joule-Thomson effect in forced flow He II (Tbath=1.675K).
The lines are guides for the eyes.

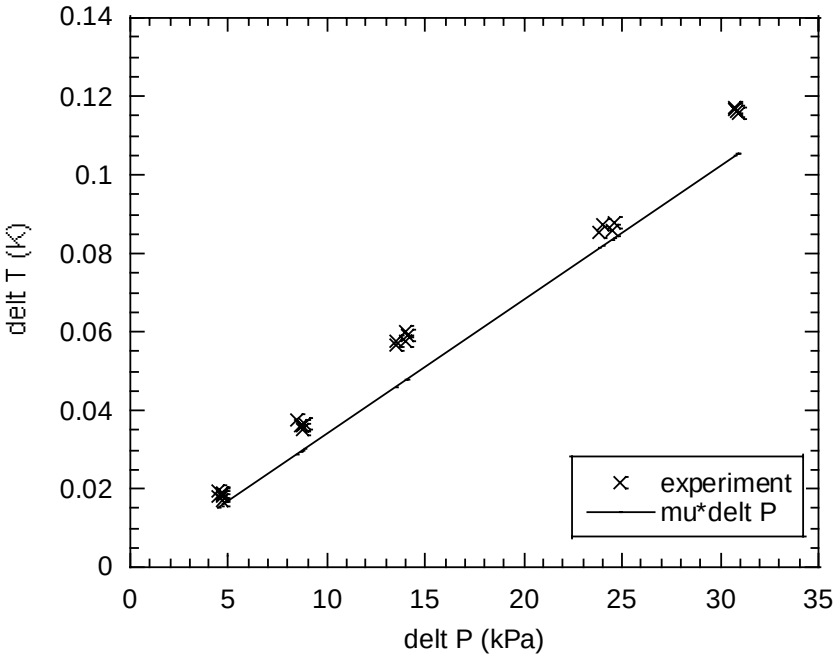

Fig.5: Difference of temperature between the last and the first thermometer versus the pressure drop between the two same locations compared to the theory (Tbath = 1.675 K).

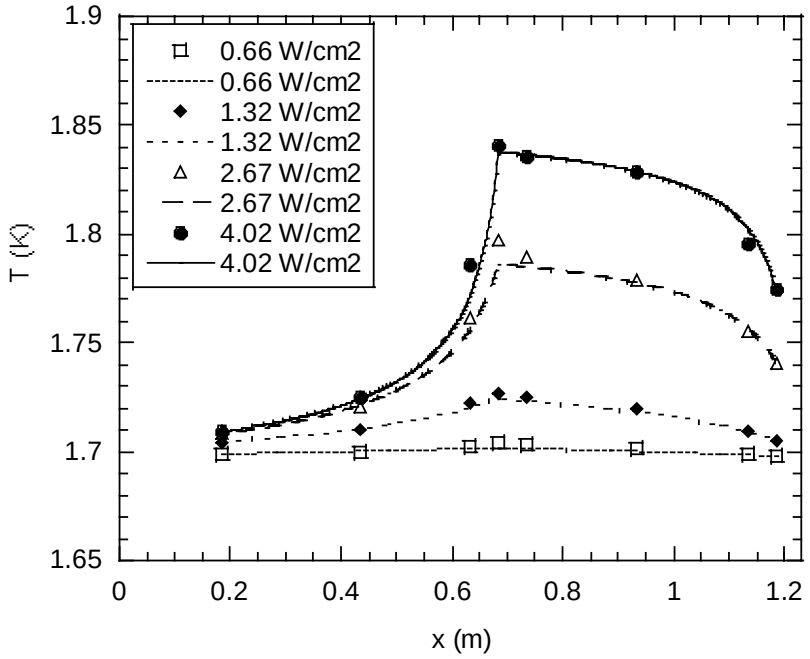

Fig.6: Heat transfer in the test section for a flow velocity of 0.52 m/s and for several heat per cross section area (Tbath=1.7K). The markers correspond to experimental results and the lines represent the numerical solution of the He II heat equation (3).

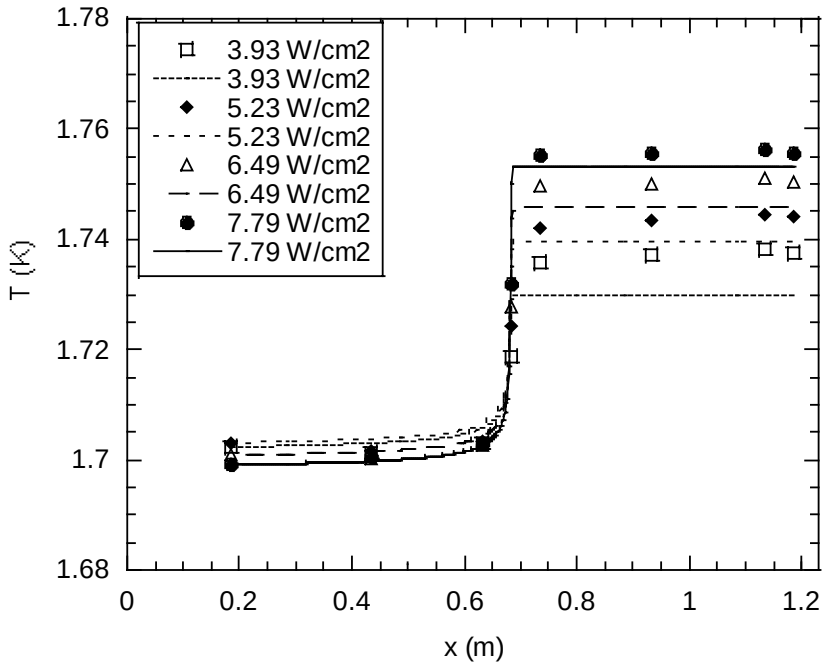

Fig.7: Heat transfer in the test section for a flow velocity of 4.14 m/s and for several heat per cross section area (Tbath=1.7K). The markers correspond to experimental results and the lines represent the numerical solution of the He II heat equation (3).

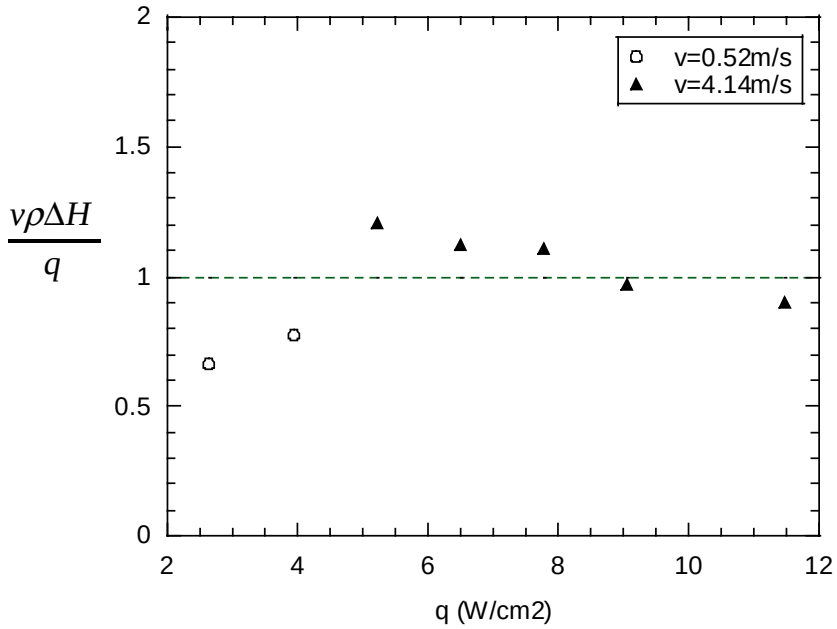

Fig.8: Heater used as a thermal flow meter (Tbath=1.7K).

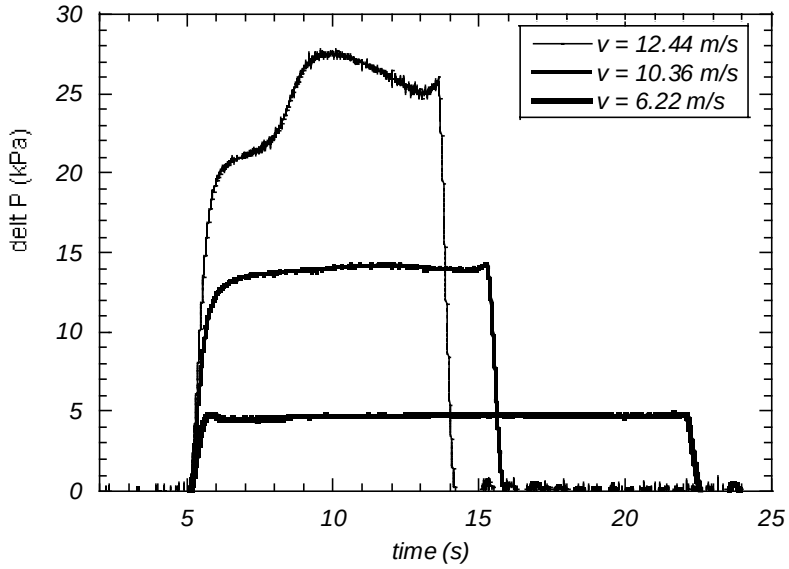

Fig.9: Evolution of the pressure drop in the test section (Tbath=1.7K).